Human Genetics (2026) 145:71
https://doi.org/10.1007/s00439-026-02864-z

ORIGINAL INVESTIGATION

Genomic characterization of historical Jinlingnan individuals: insights into genetic continuity and trans-Eurasian signals in eastern China

Shuyi Li[1] · Yuchun Wang[2] · Qu Shen[3] · Jinguo Zan[4] · Mengying Han[1] · Zishuai Huang[1] · Rui Wang[1] · Xinyi Wang[2] · Haifeng He[5] · Le Tao[6] · Hao Ma[5] · Kongyang Zhu[7] · Yetao Zou[1] · Huangzhen Huang[1] · Haodong Chen[1] · Li Jin[8] · Hui Li[1] · Chuan-Chao Wang[1,6]

Received: 17 March 2026 / Accepted: 3 August 2026

Abstract

The genetic impact of historically documented trans-Eurasian interactions in China remains poorly understood due to the scarcity of genome-wide ancient DNA data. This study presents genome-wide SNP data from 10 individuals excavated from the Jinlingnan cemetery in Zibo City, Shandong Province, dating from the Tang (618–907 AD) to the Qing (1644–1912 AD) dynasties. Although located in the agricultural heartland of eastern China rather than along major Silk Road corridors, the site provides a valuable context for investigating the integration of non-local populations into inland societies. Our analyses reveal that the Jinlingnan individuals primarily derived their ancestry from the Middle Yellow River region, showing strong genetic continuity with both contemporaneous and modern northern Chinese populations. Notably, a subset of seven individuals exhibited detectable genetic contributions from Western Eurasians or Central Asians, with proportions ranging from 1.5% to 12.1%, providing direct evidence of gene flow from trans-Eurasian interactions. Furthermore, modern Han populations in Shandong can be modeled as deriving the vast majority of their ancestry (~95%) from a Jinlingnan-related source, with a minor contribution (~5%) from southern Chinese-related groups. These results delineate the demographic history of the Jinlingnan population, characterized by foundational Central Plains continuity, localized incorporation of exogenous components, and subsequent north–south interactions. This study demonstrates that the demographic impact of trans-Eurasian exchange extended far beyond Silk Road hubs, reaching deep into inland eastern China.

Shuyi Li, Yuchun Wang and Qu Shen these authors contributed equally.

✉ Jinguo Zan
358859342@qq.com

✉ Chuan-Chao Wang
chuanchaowang@fudan.edu.cn

[1] Ministry of Education Key Laboratory of Contemporary Anthropology, Center for Evolutionary Biology, Department of Anthropology and Human Genetics, School of Life Sciences, Fudan University, Shanghai 200438, China

[2] Fujian Provincial Key Laboratory of Philosophy and Social Sciences in Bioanthropology, Institute of Anthropology, Xiamen University, Xiamen 361005, China

[3] School of Humanities, Fujian University of Technology, Fuzhou 350118, China

[4] Shandong Provincial Institute of Cultural Relics and Archaeology, Jinan 250012, China

[5] School of Life Sciences, Xiamen University, Xiamen 361102, China

[6] Institute of Forensic Science, School of Forensic Medicine and Science, Fudan University, Shanghai 200032, China

[7] Department of Evolutionary Anthropology, University of Vienna, 1030 Vienna, Austria

[8] State Key Laboratory of Genetic and Development of Complex Phenotypes, School of Life Sciences & Human Phenome Institute, Fudan University, Shanghai 200438, China

Published online: 25 August 2026

Abbreviations

SNPs	Single-nucleotide polymorphisms
HO	Human Origin
PCA	Principal components analysis
N	Neolithic
EN	Early Neolithic
MN	Middle Neolithic
LN	Late Neolithic
BA	Bronze Age
IA	Iron Age
HE	Historical era
YR	Yellow River
cal BP	Calibrated years before present
ROH	Runs of homozygosity
cM	CentiMorgans

Introduction

Recent advances in ancient DNA research have revealed a complex history of population movements and admixture within China. Ancestry associated with the Middle Yellow River region and the Neolithic Yangshao culture expanded westward into Xinjiang (Kumar et al. 2022; Yang et al. 2026; Li et al. 2025) and the Tibetan Plateau (Wang et al. 2023; Zhu et al. 2022), northward into Inner Mongolia and northern Shaanxi (Ning et al. 2020; Xiong et al. 2025, Wang et al. 2025), and southward into southwestern China and the southeastern coastal regions (Yang et al. 2020; Wang et al. 2021b; Tao et al. 2023, 2026; Zhou et al. 2025; Wan et al. 2025; Zhu et al. 2024a, b), exerting a broad and enduring genetic influence. In Xinjiang, the Bronze Age gene pool was formed through varying degrees of admixture between local ancestry related to the Xiaohe culture of the Tarim Basin and multiple exogenous sources, including Western Steppe pastoralists, populations associated with the Bactria–Margiana Archaeological Complex (BMAC), and Ancient Northeast Asian-related ancestry (Zhang et al. 2021). Compared with Bronze Age populations, Iron Age and later historical groups in Xinjiang experienced additional gene flow from Central Asia and East Asia (Kumar et al. 2022; Yang et al. 2026; Li et al. 2025). At the western end of the Hexi Corridor, a critical passage linking the Central Plains and Xinjiang, two individuals dated respectively to the Cao Wei period (220–266 AD) and the Tang dynasty (618–907 AD) have been identified as exhibiting mixed western and eastern Eurasian genetic profiles (Xiong et al. 2024). Recent ancient DNA studies from Xingfulindai (XFLD) (Lv et al. 2024) and Fudamen (Wang et al. 2025a, b) further confirmed the presence of Western Eurasian and/or Central Asian-related ancestry within the core regions of China. Nevertheless, the geographic extent and temporal dynamics of this genetic influence remain insufficiently characterized and require additional genome-wide data.

The late imperial era of China, spanning from the Tang dynasty (618–907 AD) to the Qing dynasty (1644–1912 AD), witnessed profound institutional development, economic prosperity, and extensive cultural exchange in China. The Qing dynasty (1644–1912 AD), as the final imperial period, marked the culmination of these long-term historical processes, particularly in territorial consolidation and ethnic integration. During the Tang dynasty, an outward-looking foreign policy and active engagement with polities in the Western Regions facilitated the flourishing of the Silk Road at its historical peak. Within this context, substantial numbers of so-called “Hu” populations, including Sogdian merchants, Turkic groups, and Persians, migrated into the Chinese interior along established trade routes. These incoming groups not only introduced commodities and technologies but also gradually integrated into local societies through intermarriage and long-term settlement, a process that continued in later historical periods.

These historical processes are also relevant to understanding the origins of Muslim communities in China. The Hui people, numbering approximately 10.5 million, are the largest of the ten Muslim minorities and the second-largest among the 55 officially recognized ethnic minorities in China. Historical records indicate that Islam was first introduced into China during the Tang Dynasty about 1,300 years ago, when merchants and political emissaries from Arabia, Persia, and Central Asia arrived via the Silk Road, and some eventually settled permanently. Later, during the Yuan Dynasty, additional Muslim populations from West and Central Asia migrated to China, either through forced relocation or voluntary migration (Gladney 1998; Chen 1999). Historians have therefore proposed that present-day Hui populations may largely descend from these immigrants, although anthropological studies have noted that Hui individuals generally exhibit physical features similar to those of East Asian populations.

The Jinlingnan site (Fig. 1A), located in present-day Zibo City, Shandong Province, comprises burials spanning from the Tang to the Qing dynasties. Grave goods displaying clear Sogdian cultural features have been excavated at the site. The cemetery is situated within Jinling Hui Ethnic Town (Jinling Hui Town), a settlement historically associated with Hui communities. Unlike sites situated at major nodes of the Silk Road, Jinlingnan lies within the agricultural heartland and densely populated region of eastern China, making it a unique case for investigating how foreign groups integrated into local agrarian societies distant from primary trade corridors. However, due to the lack of systematic ancient genomic data, the genetic composition

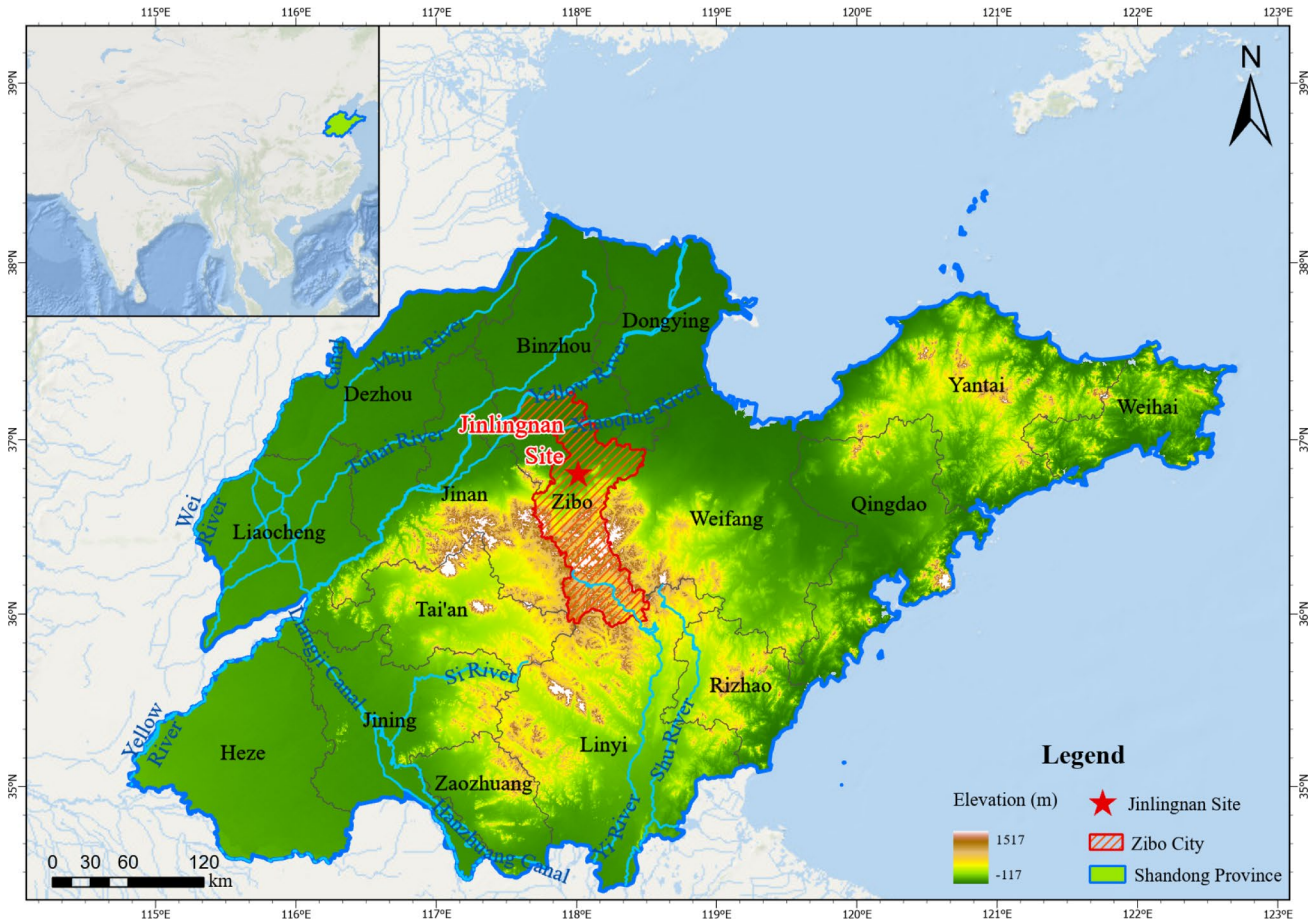

Fig. 1 Geographic location and environmental setting of the Jinlingnan site

and population history of the Jinlingnan region from the Tang to the Qing periods remain largely unknown.

To address this gap, we conducted genome-wide ancient DNA analyses of individuals from the Jinlingnan site. This study focuses on three core questions:

1. The genetic relationship between Jinlingnan populations and Neolithic Middle Yellow River-related ancestry;
2. The presence and temporal dynamics of Central Asian and Western Eurasian-related ancestry in relation to central Shandong from the Tang through the Qing periods;
3. The genetic continuity and connections between these historical populations and present-day Shandong populations.

This study provides critical genomic evidence for understanding population movements, cultural interactions, and genetic transformations in eastern China during the historical period.

Results

Ancient genomes from Jinlingnan cemetery

We obtained archaeological samples from the Jinlingnan cemetery and generated genome-wide SNP data for 16 ancient individuals using a shotgun sequencing strategy applied to double-stranded DNA libraries constructed without uracil-specific treatment. All individuals exhibited short DNA fragments typical of ancient material, with average fragment lengths ranging from 54 to 100 base pairs across genomes following adaptor trimming and read collapsing (Supplementary Data 1). The sequences displayed characteristic patterns of postmortem damage, including elevated cytosine-to-thymine substitutions at the 5′ ends and guanine-to-adenine substitutions at the 3′ ends of DNA fragments (Supplementary Fig. 1), consistent with authentic ancient DNA. To ensure data quality, we excluded individuals with high contamination (>5%), as estimated using mitochondrial DNA for all individuals and X-chromosomal data for biological males, and samples with low SNP coverage on the 1240 k panel (<30,000 SNPs). After these filtering steps,

14 individuals were retained for further analysis (Supplementary Data 1). We subsequently performed kinship analysis to assess relatedness among the Jinlingnan individuals. Among the 16 initially sequenced individuals, three familial groups were identified (Supplementary Data 2). For each related pair, we retained the individual with the higher SNP count on the 1240 k panel, resulting in a final dataset of 10 genetically unrelated individuals for downstream population genetic analyses (Supplementary Data 1). Across these 10 individuals, the proportion of human endogenous DNA ranged from 3.46 to 60.71% (Supplementary Data 1). The average depth of coverage for autosomal SNPs on the 1240 k panel ranged from 0.03 × to 4.51 × (mean: 0.83 ×) (Supplementary Data 1). The number of SNPs covered at least once on the 1240 k panel varied between 33,935 and 1,189,444 (Supplementary Data 1). Finally, we merged the newly generated Jinlingnan genomes with previously published ancient and modern genomic datasets listed in Supplementary Data 3 and 4 for comparative population genetic analyses.

Genetic Continuity between Ancient Yellow River Basin Populations and Jinlingnan

The Jinlingnan individuals (n = 10) carried mitochondrial DNA (mtDNA) lineages commonly observed in East Eurasian populations, including haplogroups F1a, B4, D4, D5, M9a, R, and A3. Among the male individuals, three possessed Y-chromosome haplogroups O1 and O2a2, which are prevalent in East Eurasia and are consistent with those previously reported in historical populations from Shandong (Shen et al. 2025).

To evaluate the genome-wide genetic structure of the Jinlingnan individuals, we performed principal component analysis (PCA) by projecting the ancient samples onto the genetic variation of present-day East Eurasian populations. The results showed that Jinlingnan individuals clustered closely with previously published Shandong historical individuals (Shandong_HE, dating from the Warring States period to the Northern Dynasties, ca. 475 BC–581 AD) and populations associated with Central Plain–related ancestry, represented by Late Neolithic Yellow River groups (YR_LN) and Late Bronze–Iron Age Yellow River groups (YR_LBIA; Fig. 2A; Supplementary Data 5). Consistent with the PCA results, unsupervised ADMIXTURE analysis indicated that Jinlingnan individuals shared similar ancestry profiles with

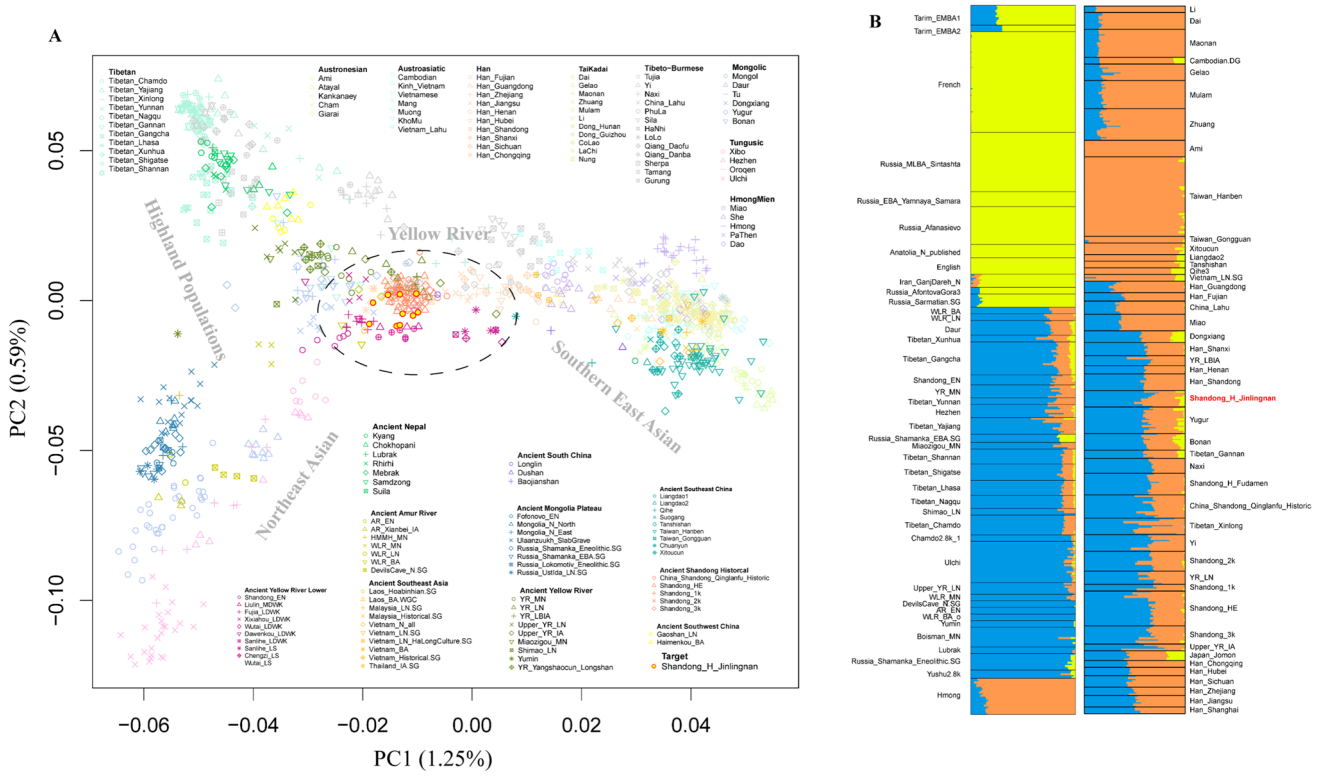

Fig. 2 Genetic structure of Shandong Jinlingnan population. **A** Principal component analysis of present-day East Asians, onto which ancient individuals were projected, onto the calculated principal components. The three clusters were visible. See also Supplementary Data 5. **B** ADMIXTURE results for the "HO" dataset at K = 3 (the lowest cross-validation error). The Shandong Jinlingnan populations were colored. See also Supplementary Data 6

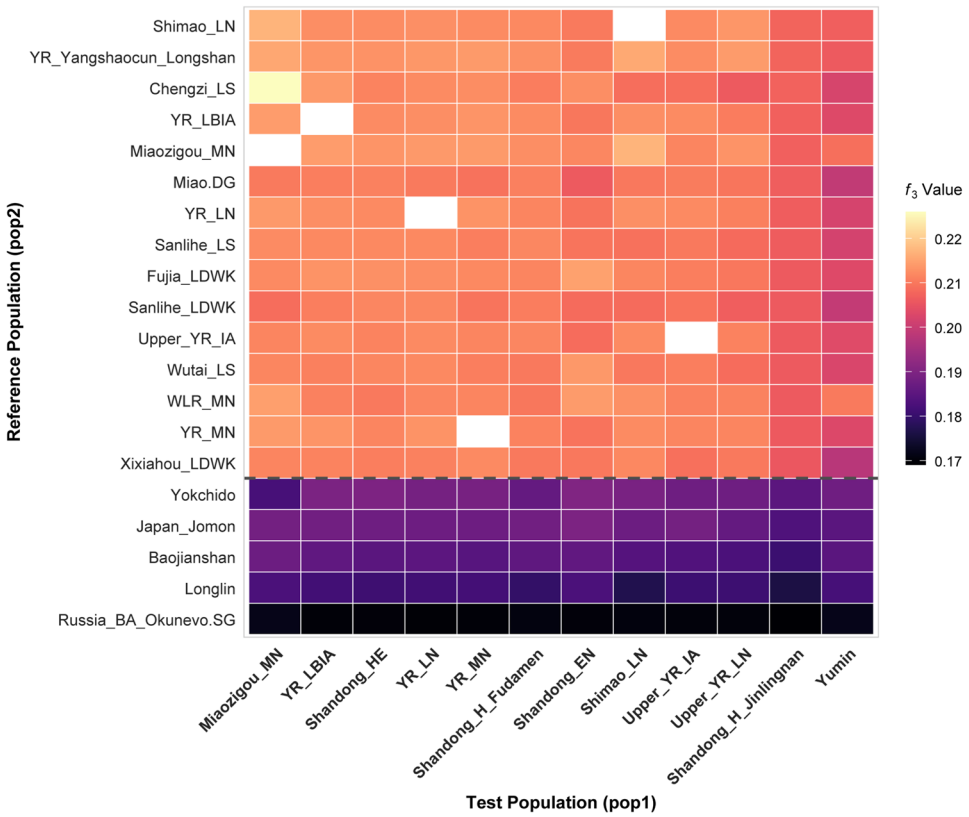

Fig. 3 **A** Outgroup f_3-statistics of f_3(X, Y; Yoruba.DG), where X represents ancient Yellow River populations and Y represents ancient East Asian reference populations. For each test population (X), heatmap values reflect the degree of genetic affinity with each reference population (Y), with higher f_3 values indicating greater shared genetic drift. Reference populations displayed are the top 15 most genetically related and bottom 5 least genetically related populations as ranked by the Jinlingnan population, separated by the dashed line. See also Supplementary Data 7. **B** The f_4-statistics in the form of f_4 (Yoruba, X; Shandong_HE, Shandong_H_Jinlingnan) tested the genetic relationships between each Jinlingnan individual and ancient Eurasian populations. In this analysis, X represents each of 194 ancient East Asian samples from different regions. See also Supplementary Data 11

Late Neolithic Yellow River Basin populations (YR_LN and YR_LBIA), Shandong_HE, and Shandong_H_Fudamen (Fig. 2B). In the model with the lowest cross-validation error (K = 3), Jinlingnan individuals were characterized by three major ancestral components: (1) a blue component predominant in Northeast Asian populations, (2) an orange component most prominent in southern East Asian populations, and (3) a yellow component enriched in Western Eurasian populations. Notably, comparative ADMIXTURE analysis of ancient Shandong populations revealed differences between Jinlingnan and Shandong_HE individuals. Specifically, Jinlingnan individuals exhibited a more pronounced yellow (Western Eurasian–related) component than both Shandong_HE and Shandong_Fudamen individuals (Fig. 2B; Supplementary Data 6). These observations were further supported by Outgroup-f_3 statistics in the form of f_3 (Ancient Yellow River populations, Y; Yoruba), where Y represented 70 ancient East Asians from different regions, demonstrating that the Jinlingnan population shared similar levels of genetic affinity with other ancient populations from the middle and lower Yellow River regions (Fig. 3A; Supplementary Data 7). Additionally, Outgroup-f_3 statistics of the form f_3 (Shandong_H_Jinlingnan, X; Yoruba) indicated that Jinlingnan individuals were most closely related to ancient populations from Foyemiaowan in Gansu and Chengzi in Shandong (Supplementary Fig. 2; Supplementary Data 8).

Pairwise *qpWave* analysis (Supplementary Fig. 3) indicated overall genetic homogeneity among the Jinlingnan individuals, except for individual SD-1-20. Furthermore, additional pairwise *qpWave* tests demonstrated that several Jinlingnan individuals could not be statistically distinguished from Shandong_HE and other Yellow River groups, including YR_LN, YR_LBIA, and Late Iron Age groups from the Upper Yellow River (Upper_YR_IA), as indicated by non-significant p-values ($p > 0.05$) (Supplementary Fig. 4; Supplementary Data 9). These results further support the close genetic connections between the Jinlingnan population and ancient populations from the Yellow River region.

Western Eurasian/Central Asian–related genetic contributions to the Jinlingnan population

To quantitatively assess whether the Shandong_H_Jinlingnan individuals derived from the same source population as previously published historical-era individuals from Shandong (represented by the larger Shandong_HE dataset), we calculated f_4 statistics of the form f_4 (Yoruba, X; Shandong_HE, Shandong_H_Jinlingnan, n = 10). Results indicated that several Western Eurasian- and Central Asian-related populations, including Uzbekistan_BA_SappaliTepe, Russia_Afanasievo, and Russia_MLBA_Sintashta, exhibited significantly higher genetic

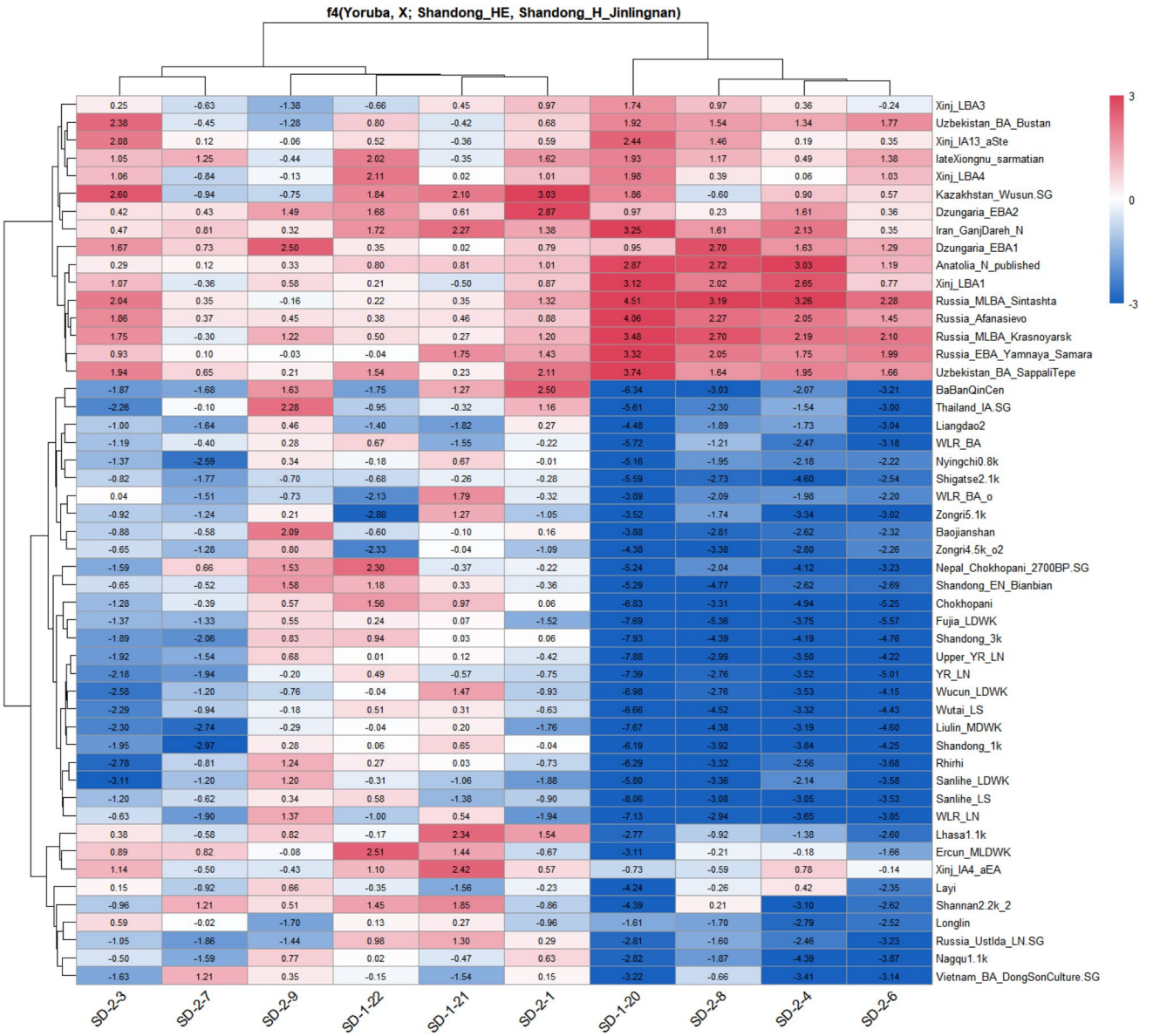

Fig. 3 (continued)

affinity to Shandong_H_Jinlingnan than to Shandong_HE (Supplementary Data 10; Supplementary Fig. 5). We further computed f_4 statistics in the form f_4 (Yoruba, X; Shandong_HE, each Shandong_H_Jinlingnan individual) (Fig. 3B; Supplementary Fig. 5; Supplementary Data 11). To detect even marginal yet statistically reliable signals of non–Yellow River–related ancestry in Shandong_H_Jinlingnan individuals, we adopted a significance threshold of $|Z| \geq 2$. Notably, seven out of ten individuals showed significantly greater allele sharing with diverse Western Eurasian/Central Asian populations compared to Shandong_HE. To determine whether Shandong_HE-related ancestry alone could sufficiently explain the genetic profiles of the ten Shandong_H_Jinlingnan individuals, we first performed *qpWave* analysis by sequentially incorporating populations that yielded significant f_4 results into the outgroup set (Supplementary Data 11). The one-way Shandong_HE model failed for three individuals (SD-1-20, SD-2-4, and SD-2-6) (Supplementary Data 12), indicating that a single-source model was insufficient for these cases.

Based on these findings, we selected populations (Supplementary Data 10) exhibiting excess allele sharing (Russia_MLBA_Sintashta and Uzbekistan_BA_SappaliTepe) as candidate secondary sources and conducted two-way admixture modeling using *qpAdm* (Supplementary Fig. 6A; Supplementary Data 13). The proposed two-source models were feasible for all seven individuals who demonstrated significant Western Eurasian/Central Asian affinity in the f_4

analysis. Moreover, the two-source models provided a better fit than the single-source Shandong_HE models. Estimated Western Eurasian/Central Asian–related ancestry proportions varied across individuals: SD-1-21 (Song Dynasty, 990-671 cal BP) and SD-2-1 (Yuan Dynasty, 679-582 cal BP) exhibited approximately 2% Western Eurasian/Central Asian–related ancestry; SD-2-4, SD-2-6 and SD-2-8 (Qing Dynasty, 285-29 cal BP) showed approximately 5%; SD-1-20 and SD-2-3 (Qing Dynasty, 264-24 cal BP), displayed approximately 11%. Accordingly, we classified the seven Shandong_H_Jinlingnan individuals exhibiting detectable Western Eurasian/Central Asian–related ancestry as the "Shandong_H_Jinlingnan_2" group (n = 7), and the remaining three individuals as the "Shandong_H_Jinlingnan_1" group (n = 3). For the Shandong_H_Jinlingnan_1 group, all one-way Shandong_HE *qpWave* models remained statistically supported, even when populations showing excess allele sharing were included in the outgroup set (Supplementary Data 14; Supplementary Data 15). These results indicate that Shandong_HE-related ancestry adequately explains the genetic profiles of the Shandong_H_Jinlingnan_1 individuals.

Temporal estimation of admixture and demographic inference in the Jinlingnan population

We applied the DATES software to estimate the timing of admixture in the Shandong_H_Jinlingnan_2_Qing individual. Assuming that the Western Eurasian/Central Asian–related ancestry resulted from a single-pulse admixture event and using Shandong_HE as a proxy for the local ancestral source, the admixture event was dated to 21.1 ± 3.6 generations prior to this individual's lifetime (Supplementary Data 16; Supplementary Fig. 7). Assuming a generation time of 28 years, this corresponds to 592 ± 101 years before the individual's lifetime. The individual is radiocarbon dated to 285–29 and 264–24 cal BP; using the midpoint of these calibrated ranges as an approximation places the individual at approximately AD 1817. Based on this estimate, the admixture event is inferred to have occurred around AD 1225, with an estimated range of AD 1124–1326. This timeframe spans the late Southern Song Dynasty to the Yuan Dynasty. We note, however, that these estimates are based on a simplified single-pulse admixture model. In reality, the genetic interaction between East and West Eurasian populations was likely a continuous or multi-wave process. Since LD-based methods like DATES tend to capture a weighted average or the most recent significant admixture signal, our results likely reflect a recent phase of contact, and the true initiation of these interactions may significantly predate these calculated estimates.

To further explore the demographic history of the Jinlingnan population, we analyzed runs of homozygosity (ROH), which represent contiguous genomic regions identical by descent due to shared ancestry. A cumulative length of long ROH segments (> 20 cM) exceeding 50 cM is indicative of recent consanguinity, reflecting parental relatedness. In contrast, populations with relatively small effective population sizes are expected to exhibit an excess of short ROH segments (4–8 cM). We applied hapROH to infer ROH patterns for Jinlingnan individuals (Supplementary Fig. 8). Several individuals (SD-1-21, SD-2-4, SD-2-6, and SD-2-8) displayed continuous short ROH segments, consistent with ancestry derived from populations characterized by relatively small effective population sizes. No evidence of excessively long ROH segments was observed, suggesting the absence of recent close-kin inbreeding.

Genetic continuity and affinity between Jinlingnan and Present-Day Han Chinese

To assess genetic relationships between Shandong_H_Jinlingnan and present-day Han Chinese and ethnic minority populations, we performed pairwise *qpWave* analyses (Supplementary Fig. 9; Supplementary Data 17). Significant genetic homogeneity (P > 0.01) was observed among Shandong_H_Jinlingnan_1, Han_Shanghai, Han_Shandong, and other Han Chinese populations. Outgroup-f_3 statistics (Supplementary Data 18) revealed that Shandong_H_Jinlingnan_1 exhibited the greatest genetic affinity to Central Chinese Han populations, represented by Han_Zhejiang, Han_Shanghai, and Han_Jiangsu, rather than to Han_Shandong. Symmetric f_4 statistics of the form f_4(Yoruba, Shandong_H_Jinlingnan_1; Han_i, Han_j) further confirmed that Shandong_H_Jinlingnan_1 shared more alleles with Central Chinese Han populations than with Han_Shandong (Supplementary Data 19). Subsequent *qpAdm* modeling demonstrated that present-day Shandong Han Chinese are best characterized as a two-way admixture comprising approximately 95% Shandong_H_Jinlingnan_1–related ancestry and 4–5% southern Chinese–related ancestry, represented by BaBanQinCen (Wang et al. 2021b) (Supplementary Fig. 10; Supplementary Data 20).

Discussion

The Yellow River basin is a core region for the origin and early development of Chinese civilization. Recent ancient genomic studies have revealed that the Middle Yellow River Neolithic population (YR_LN) had a profound impact on the genetic structure of historical populations throughout the Yellow River basin and broader East Asia (Xiong et al. 2024,

Ma et al. 2025, Shen et al. 2025, Cooke et al. 2021, Wang F et al. 2024, Zhou et al. 2026, Tang et al. 2026, He et al. 2025, Sun et al. 2025, Li et al. 2024). The Shandong region, in particular, has experienced continuous gene flow from the Central Plains since the Neolithic (Du et al. 2024; Fang et al. 2025). Consequently, historical populations in Shandong universally exhibit a high degree of genetic homogeneity with those of the Middle Yellow River (Shen et al. 2025, Qiu et al. 2026, Wang et al. 2024, Ji et al. 2025), demonstrating long-term and stable genetic continuity. Our genomic analysis indicates that YR_LN ancestry is the dominant ancestral component within the Jinlingnan group, underscoring the population's primary genetic affinity to the broader Middle Yellow River tradition. Although two-way admixture models suggest a minor Western Eurasian–related component in a subset of individuals, the fundamental genomic structure of the Jinlingnan population remains closely aligned with the Yellow River genetic lineage. This pattern confirms that the primary gene pool of inland Shandong was characterized by deep genetic continuity, with Yellow River-related ancestry serving as a consistent genetic backbone through successive historical periods. Thus, the overall genetic profile of Jinlingnan reflects a predominantly Yellow River–derived population structure with superimposed signals of limited external gene flow. This dual pattern, strong affinity with Middle Yellow River populations alongside low-level Western Eurasian–related ancestry, highlights the demographic complexity of inland Shandong during the historical period. It suggests that long-term regional genetic stability coexisted with episodes of interregional interaction.

Previous historical and genomic research indicates that trans-Eurasian interactions were not limited to cultural exchange but also involved tangible demographic processes (Yao et al. 2021; Xue et al. 2025). Historical records document the sustained migration of Sogdian and other Central Asian groups into North China from the Eastern Han through the Northern Dynasties (Liu 2023), with the establishment of diaspora communities in the Hexi Corridor, the Central Plains, and northern frontier regions (Nodirabegim 2021; Liu 2023). These groups actively participated in trade, political administration, and cultural transmission and were progressively incorporated into local societies (Nodirabegim 2021; Liu 2023). Genomic studies from northwestern China further corroborate these historical accounts (Yao et al. 2021). Modern northwestern Han populations have been shown to derive predominantly from Yellow River–related ancestry (Ning et al. 2020; Wang et al. 2021a; Yang et al. 2020; Yao et al. 2021), yet consistently harbor a minor but detectable Western Eurasian component, dated primarily to the historical period and likely associated with intensified Silk Road interactions (Loh et al. 2013; Yao et al. 2021). Ancient DNA evidence from Xinjiang provides a broader temporal framework for such west–east genetic exchanges (Xue et al. 2025). From the Bronze Age onward, Xinjiang served as a major hub for Eurasian population interaction, characterized by recurrent admixture among steppe pastoralists, BMAC-related agriculturalists, and East Asian groups (Jeong et al. 2020; Frachetti 2013; Xue et al. 2025). During the Iron Age and Historical Era, increasing Yellow River–related ancestry in Xinjiang populations reflects bidirectional gene flow facilitated by expanding communication networks (Yang et al. 2025; Li et al. 2025; Allen et al. 2022). Collectively, these studies indicate that low-level Western Eurasian–related ancestry observed in inland northern China should be interpreted within the broader context of long-term, spatially heterogeneous trans-Eurasian demographic processes rather than as isolated or anomalous events (Yao et al. 2021; Xue et al. 2025).

Concurrently, we detected consistent but low-level signals of Western Eurasian/Central Asian–related ancestry within the Jinlingnan population. This component, present in seven of the ten individuals, exhibits moderate variation in its proportions. The highest levels (~11%) are observed in several Qing Dynasty individuals (SD-1-20 and SD-2-3), followed by intermediate levels (~5%) in other Qing individuals (SD-2-6, SD-2-8, and SD-2-4), while the lowest proportions (~2%) occur in the Song (SD-1-21) and Yuan (SD-2-1) individuals. This distribution does not support a simple model of progressive dilution over time, but instead suggests a more complex demographic history. Admixture dating using DATES further refines this interpretation. Based on the Shandong_H_Jinlingnan_2_Qing individual, the admixture event is estimated to have occurred 592 ± 101 years prior to the individual's lifetime, corresponding to a timeframe of AD 1124–1326. This interval spans the late Southern Song Dynasty to the Yuan Dynasty, indicating that the introduction of Western Eurasian/Central Asian–related ancestry likely predates the sampled Qing individuals by several centuries. The temporal offset between the inferred admixture event and the later individuals carrying elevated proportions argues against a recent or single-wave gene flow scenario. Instead, it supports a model in which earlier admixture is followed by differential retention or reintroduction of this ancestry component over time. Despite this clear autosomal signal, all individuals carry exclusively East Asian mitochondrial and Y-chromosomal haplogroups. This discordance is consistent with a scenario of multi-generational admixture, in which initial exogenous gene flow was followed by prolonged integration into a predominantly East Asian gene pool, leading to the stochastic loss of non-local uniparental lineages while retaining low-level autosomal ancestry.

Although X-chromosome-based *qpAdm* modeling was attempted to evaluate potential sex-biased admixture, the

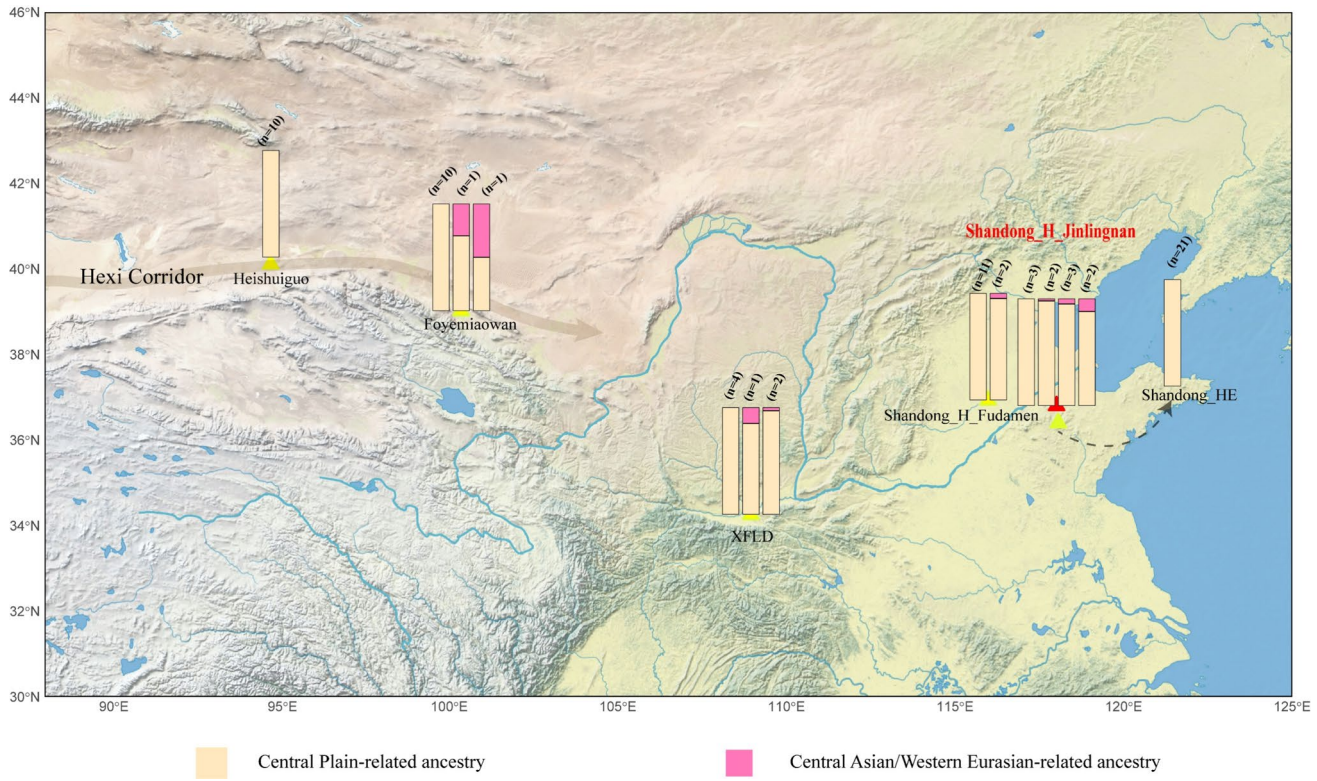

Fig. 4 Ancestry profile of historical era populations from Hexi Corridor, Central Plain, and Shandong, inferred by *qpAdm*-based modelling. Each coloured block represents the proportion of ancestry derived from a corresponding source in the legend, with error bars representing ± 1 standard error (SE). Numbers in brackets denote the sample size for each group. The Jinlingnan individuals are categorized into four subgroups (3–2-3–2) based on their specific levels of Western Eurasian/Central Asian-related ancestry: the first group (n = 3) shows 0% exogenous ancestry; the second (n = 2) exhibits ~ 2% (SD-1–21, SD-2–1); the third (n = 3) shows ~ 5% (SD-2–4, SD-2–6, SD-2–8); and the fourth (n = 2) displays ~ 11% (SD-1–20, SD-2–3). See also Supplementary Data 13 for further details

resulting ancestry estimates were unstable and poorly constrained, precluding a reliable comparison with autosomal results (Supplementary Data 21).

Compared with contemporaneous populations from XFLD (3 out of 5 individuals with ~ 3–15% western ancestry) and Fudamen (2 out of 17 individuals with ~ 5% western ancestry), the Jinlingnan population shows both a higher frequency of individuals carrying Western Eurasian–related ancestry (7 out of 10 individuals, with proportions ranging from ~ 2% to ~ 11%) and a more pronounced overall genetic contribution. (Fig. 4). Following the multidisciplinary 'triangulation' approach that integrates genetic, archaeological, and historical-linguistic evidence (Robbeets et al. 2021; Savelyev and Robbeets 2020), a unified analysis provides critical insights into the formation and demographic history of the Jinlingnan population. Although located in eastern China and not a primary Silk Road center, historical records underscore Jinlingnan's longstanding strategic significance. Established during the early Tang Dynasty near crucial mountain passes on an east–west route, Jinlingnan served as an important transportation nexus, as evidenced by the founding of 'Jinling Post Station' (金岭驿) and its later recognition as 'Jinling Town' (金岭镇) in the Five Dynasties period. This tradition of connectivity persisted for centuries. By the late Yuan and early Ming dynasties, Jinlingnan had developed into a prominent Hui town (金岭回族镇), with residents engaged primarily in commerce and various trades. Integrating genetic data reveals the enduring presence of Western Eurasian/Central Asian-related ancestry in the population. Contrary to expectations of gradual dilution following a single admixture event, genetic evidence indicates lower levels of Western Eurasian ancestry in Song–Yuan individuals and higher proportions in Qing dynasty individuals. Furthermore, archaeological findings reveal distinct differences in mortuary practices between these periods. Song–Yuan burials demonstrate full Sinicization, with brick-vaulted chambers, south-facing entrances, typical Song–Yuan ceramic assemblages (瓷器组合), copper coins (铜钱) as grave goods, and irregular multiple interments in single chambers, characteristic of secondary burial practices (二次葬). In contrast, burials from the Qing dynasty, including individuals M11 (SD-2-3), M12 (SD-2-4), M14 (SD-2-6), M15 (SD-2-7), M16 (SD-1-20), and M18 (SD-2-8), exhibit Islamic mortuary practices (Yang 1999) such

as rectangular pit-cave tombs, absence of grave goods and coffins, and westward orientation of the deceased. Genetic analysis of these individuals reveals no evidence of recent close-kin unions or systematic inbreeding, as indicated by the absence of long runs of homozygosity (ROH), whereas short ROH segments suggest ancestry from relatively small communities. The differences in Western Eurasian ancestry and burial practices indicate a complex demographic history driven by structured gene flow, repeated migrations, population substructure, and random fluctuations in ancestry. Rather than reflecting a single episode of admixture in the Song–Yuan period, the patterns are consistent with multiple episodes of Western Eurasian-related migration and subsequent reshuffling, resulting in a heterogeneous distribution of ancestry. From a historical-linguistic perspective, the evolution of the Hui population involved a gradual language shift, with Persian and Arabic originally spoken by early Muslim settlers, and Chinese eventually adopted over centuries. Even after the transition, the resulting "Huihui speech" (回回话) (Ying-sheng 2003) retained a substantial lexical substrate from Persian and Arabic, especially in religious, familial, and dietary contexts. This linguistic retention echoes the persistence of Western Eurasian ancestry, reflecting the selective integration of exogenous elements into local cultural and genetic traditions. Overall, the combined genetic, archaeological, and linguistic evidence points to Jinlingnan as a significant inland node of trans-Eurasian interaction, with ongoing and structured integration processes rather than simple assimilation or isolation. The results demonstrate that the biological consequences of these long-distance interactions extended well beyond the principal Silk Road corridors, deeply influencing local populations in strategic inland hubs like Jinlingnan.

We further compared the ancient Jinlingnan population with modern Han Chinese groups to investigate local genetic continuity. The individuals in the Shandong_H_Jinlingnan_1 group show genetic affinity with modern northern and central Han Chinese, consistent with the predominant local ancestry, suggesting a degree of genetic stability in these populations since the historical period. In contrast, present-day Shandong Han are best modeled as a mixture of a predominant ancestry source related to the Jinlingnan population (~95%) and a smaller southern Chinese–related component (~5%). This pattern suggests that the historical Shandong gene pool forms a major ancestral substrate for contemporary inhabitants. At the same time, subsequent north–south population movements also contributed to shaping their modern genetic profile.

In conclusion, our study provides a genomic snapshot of individuals from the Jinlingnan site, offering an informative perspective on the genetic landscape of historical inland Shandong. While these findings from a single cemetery cannot represent the entire regional population, they provide direct evidence of individuals with minor exogenous ancestry within a predominantly Yellow River–related genetic background. This site-specific study illustrates a complex demographic process involving long-term genetic stability from the Central Plains, interspersed with localized signals of external genetic contributions. These results contribute to our understanding of the fine-scale genetic structure in eastern China. However, broader archaeogenomic sampling across more diverse temporal and geographic contexts remains necessary to fully characterize the regional population dynamics and the formation of the modern Han Chinese.

Methods

Archaeological information for Jinlingnan (金岭南)

The specimens for this study were recovered from the Jinlingnan cemetery in Zibo City, Shandong Province. In 2023, the Shandong Provincial Institute of Cultural Relics and Archaeology conducted a rescue excavation, uncovering 18 tombs. Based on the typological analysis of unearthed artifacts, epitaph records, and radiocarbon dating, these tombs represent a continuous chronological span from the Tang to Qing Dynasties. Among the 16 individuals sampled from this site, the majority are associated with the Qing Dynasty, while others date to the Qing, Song, and Yuan periods. This cohort provides a unique opportunity to examine the genetic history of historical populations in the region across several centuries. Detailed archaeological information is provided in Supplementary Data 1.

Radiocarbon dating

We performed accelerator mass spectrometry (AMS) radiocarbon dating on collagen extracted from bone and tooth samples. Samples were first physically pretreated by ultrasonication, grinding, and sieving to obtain a 0.5–1 mm fraction. Subsequently, we purified the collagen using a standard acid–base-acid (ABA) protocol (0.5 M HCl, 0.1–0.2 M NaOH, then 0.5 M HCl). The extracted collagen was then gelatinized (pH 3, 70 °C, 20 h), filtered, and freeze-dried. Quality control was essential; only collagen meeting strict criteria (yield > 1%; atomic C: N ratio of 2.9–3.5) was selected for dating (van Klinken 1999). The qualified collagen was combusted to CO_2, which was then purified and graphitized. These graphite samples were analyzed at the Guangzhou Institute of Geochemistry (Chinese Academy of Sciences) on a 0.5 MeV NEC compact AMS (Zhu et al. 2015). Finally, we calibrated the resulting conventional

radiocarbon ages against the IntCal20 curve (Knapp et al. 2011) in OxCal (Ramsey and Lee 2013) to obtain calendar dates.

Ancient DNA extraction and sequencing

A total of 16 skeletal specimens were subjected to experimental analysis in this study. All experimental procedures were conducted in the specially designed ancient DNA cleanroom laboratory at Xiamen University (Knapp et al. 2012; Llamas et al. 2017; Zhu et al. 2024a, b). We utilized 75% ethanol and 10% sodium hypochlorite (NaClO) to eliminate external contaminants. After surface abrasion and ultraviolet (UV) radiation treatment, we employed a drill bit to obtain inner core bone powder ranging from 130 to 230 mg. For each 100 mg of bone powder, we added 1 ml of 0.5 M EDTA and 1 µl of 20 mg/ml proteinase K, followed by incubation at 37 °C on a shaker at 300 rpm for 20 h. We used the MinElute System (Qiagen, Germany) to obtain concentrated DNA fragments. We prepared double-stranded libraries using the NEBNext® Ultra™ II DNA Library Prep Kit, paired with in-house designed sticky-end adaptors. We then sequenced the libraries on the DNBSEQ-T7 platform.

DNA sequence data processing

Using AdapterRemoval (version 2.3.0) (Schubert et al. 2016), we removed adaptors from both read pairs, trimmed bases at 5'/3' termini with quality scores ≤ 20 and ambiguous bases (N) (–trimns –trimqualities –minquality 20), collapsed forward and reverse reads (–collapse), and discarded reads shorter than 30 bp. Collapsed reads were aligned against the human reference genome hs37d5 (GRCh37 with decoy sequences) using the aln and samse modules in the Burrows-Wheeler Aligner (BWA) programme (version 0.7.17-r1188)(Li and Durbin 2010), with parameters '-l 1024' (seeding disabled) and '-n 0.01' (additional mismatches allowed). BAM files were sorted and indexed using Samtools (version 1.21) (Li et al. 2009) before being used to remove PCR duplicates using dedup (version v0.12.5) (Peltzer et al. 2016). BAM data were filtered with Samtools (version 1.21) (Li et al. 2009) with a minimum Phred-scaled mapping quality score of 30.

Data quality control

We used a variety of methods to assess the authenticity of the ancient DNA. First, we used mapDamage (version 2.0.8) (Ginolhac et al. 2011) to compute the postmortem damage pattern. We determined if each library had > 10% C-to-T misincorporations at 5' termini and > 10% G-to-A misincorporations at 3' termini, as is expected for double-stranded libraries. Second, we estimated the contamination rate. To calculate the mtDNA contamination rate, (1) we used the schmutzi.pl module in Schmutzi software (Renaud et al. 2015) and the contaminant database developed for Eurasian samples from share/schmutzi/alleleFreqMT/eurasian/freqs; and (2) we followed the pipeline posted in https://github.com/mnievesc/Ancient_mtDNA_Pipeline/blob/master/MT_DataAnalysis_Pipeline.sh to conduct contamMix (Fu et al. 2013)-related analysis. The X-chromosomal contamination rate was calculated for males using the contamination module in ANGSD software (version 0.931) (Korneliussen et al. 2014). We used the HapMap resources for CHB (Han Chinese in Beijing) and the ANGSD software to identify X-chromosomal polymorphic sites. We focused our investigation on the non-recombining part of the X chromosome (X:5,000,000–154,900,000). The library was treated as contaminated when mtDNA contamination exceeded 5%, except when nuclear DNA contamination was < 5% on the X chromosome in males.

Biological sex determination

An individual with one X chromosome and one Y chromosome was designated as "male," whereas an individual with two X chromosomes was designated as "female." Rx and Ry statistics (Mittnik et al. 2016; de Flamingh et al. 2020) were computed to estimate the biological sex of the samples from shotgun data.

Genotyping

We used the trimBam module in BamUtil (version 1.0.14) (Jun et al. 2015) to mask 8 bp from both ends to reduce bias caused by ancient DNA deamination. We randomly selected one high-quality base (–q 30 and –Q 30) as a pseudo-haploid using pileupcaller (https://github.com/stschiff/sequenceTools).

Estimation of genetic relatedness

We first applied PLINK software (version 1.9) to exclude non-polymorphic and low-frequency variants (–maf 0.01). We then applied the default parameters of the READv2 software (Alacamli et al. 2024) to estimate the biological relatedness between each pair of Jinlingnan individuals.

Uniparental haplogroup assignment

We produced mitochondrial consensus sequences of quality ≥ 20 using the log2fasta tool in Schmutzi software (Renaud et al. 2015). Y-chromosomal and mitochondrial haplogroups were assigned by Yleaf (version 3.2.1) (Ralf et

al. 2018) with "–reference_genome hg19 -r 1 -aDNA -old" option, haploGrouper (Jagadeesan et al. 2021) and Haplogrep (version 3) software (Weissensteiner et al. 2016), respectively. Here we describe the manual check for the Y chromosomal haplogroup assignment for 3 males:

- Individual SD-1–22 was assigned to haplogroup O2a-1b1a1a based on the presence of the derived allele at O-CTS12658, with ancestral alleles observed at downstream markers F18858, FGC66019, F592, MF7954, F723, FGC60777, and MF7064, as determined by Yleaf analysis. This result indicates classification within the O-CTS12658 lineage but not in any of the tested downstream subclades.
- Individual SD-2–6 was assigned to haplogroup O1a1a1a1a1a1a1 based on the presence of the derived allele at O-A12440, with ancestral alleles observed at downstream markers F18460, ACT1077, ACT5224, ACT6715, MF20192, Y156896, MF6062, MF6065, MF6481, and MF20371, as determined by Yleaf analysis. This result indicates classification within the O-A12440 lineage but not in any of the tested downstream subclades.
- Individual SD-2–7 was assigned to haplogroup O1 based on the presence of the derived allele at O-F75, with ancestral alleles observed at downstream markers MF6409, Y137081, Y146786, MF19965, ACT1103, Z23437, K644, F3288, F4233, CTS1456, and F2315, as determined by Yleaf analysis. This result indicates classification within the O-F75 lineage but not in any of the tested downstream subclades.

Data merging

We merged Jinlingnan samples with published genome-wide SNP data of present-day and ancient Eurasians using the mergeit function in EIGENSOFT software (Patterson et al. 2012). The information on co-analysed ancient and modern genomes is listed in Supplementary Data 3 and 4. Two datasets were used in our analysis: (1) We merged Fudamen data with the 1240 k dataset curated by The Allen Ancient DNA Resource (AADR) (Mallick et al. 2024), which covered ancient DNA data with maximum SNP sites (1,135,618). (2) We merged Fudamen data with the Human Origin (HO) dataset curated by The Allen Ancient DNA Resource (AADR) (Mallick et al. 2024), which covered ancient DNA data with overlapped SNP sites between 1240 k and the HO SNP panel (593,120), as well as present-day Eurasians genotyped on the HO SNP chip.

Principal components analysis (PCA)

We ran PCA on the HO dataset using the smartpca (version 18140) algorithm in EIGENSOFT software (Patterson et al. 2012) with the options "lsqproject: YES", "numoutlier-iter:0", and "shrinkmode: YES". We employed the "lsqproject: YES" option to project all ancient genomes onto the PC spaces calculated with the modern genomes.

Unsupervised ADMIXTURE

We pruned the strong linkage disequilibrium using PLINK software (version 1.9) (Purcell et al. 2007) with option "–indep-pairwise 200 25 0.4" on the merge Human Origin dataset. We ran the unsupervised ADMIXTURE using the ADMIXTURE software v1.3.0 (Alexander et al. 2009) with default parameters, setting K to range from 2 to 10.

F statistics

We applied qp3pop (version 420) from the ADMIXTOOLS software (Patterson et al. 2012) with the option "inbred: YES" To calculate Outgroup-f_3 in the form of f_3(A, B; Yoruba). We used qpDstat (version 751) from the ADMIXTOOLS software44 with the option "f4mode: YES" to calculate f_4 statistics in the form of f_4 (Yoruba, A; B, C). Standard error (Std.err) was calculated using 5 cM block jackknifing as implemented in the ADMIXTOOLS software (Patterson et al. 2012).

Admixture modelling using *qpAdm*

We modelled our genomes as an admixture of two source populations and estimated the proportions of ancestry using *qpAdm* (version 810) in ADMIXTOOLS software (Patterson et al. 2012), with settings "details: YES" and "allsnps: YES". We chose the following populations as the base outgroups: Mbuti.DG, Russia_MA1_HG.SG, Tianyuan, Mongolia_N_East, Russia_EHG, Dushan, Taiwan_Hanben, Lubrak. All the conditions listed below should be satisfied: (1) Coefficient>0 and Coefficient$\pm$Std.err>0; (2) p-value>0.01; (3) p-value for the nested model<0.05.

Estimating the admixture dates

We applied the DATES algorithm (version 753) (Chintalapati, Patterson, and Moorjani 2022) under a single-pulse admixture model to date the admixture in a single ancient genome. We used the following parameters: "binsize: 0.001", "maxdis: 1", "runmode: 1", "mincunt: 1", and "lovaifit: 0.45". We assumed 29 years per generation44.

Runs of homozygosity

ROH refers to segments of the genome where the two chromosomes in an individual are identical to each other owing to recent common ancestry. Therefore, the presence of long ROH segments strongly suggests that an individual's parents are related. We applied the hapROH method using the Python library hapROH (Ringbauer et al. 2021) with default parameters. The method was developed to identify ROH from low-coverage genotype data typical of ancient DNA and remains robust enough to identify ROH for individuals with coverage as low as 0.5×. We reported the total sum of ROH longer than 4, 8, 12 and 20 cM and visualized the results using Datagraph.

Statistics and reproducibility

Modern human contamination rates were estimated at < 1% using ContamMix and ANGSD. Detailed information on the statistical analyses carried out as described in the 'Methods' section. All analyses can be reproduced by accessing the associated data linked in the Data availability statement.

Supplementary Information The online version contains supplementary material available at https://doi.org/10.1007/s00439-026-02864-z.

Acknowledgements The work was funded by the National Key Research and Development Program (2024YFC3306701).

Author contributions C.C.W. conceived and supervised the project. J.Z. provided the materials and resources. Y.W., Q.S., H.M., L.T., and H.H. performed the wet laboratory work. S.L., R.W., Z.H., Y.Z., H.H., H.C., and K.Z. performed the genetic data analysis and prepared the figures. M.H. performed the radiocarbon dating of ancient samples. S.L. and C.C.W. wrote and edited the manuscript. H.L. was involved in the discussion. All authors contributed to the article and approved the final version for submission.

Code availability No new code and sequence analysis methods were developed. Details on the analysis settings are provided in the 'Methods' section.

Data Availability The BAM files reported in this paper have been deposited in the Genome Sequence Archive in the National Genomics Data Center, China National Center for Bioinformation/Beijing Institute of Genomics, Chinese Academy of Sciences (GSA-Human: HRA020278). All other data are available from the corresponding author on reasonable request.

Declarations

Conflict of interest The authors declare that they have no conflict of interest.

Ethical approval The procedures related to the study of human subjects and the analysis of archaeological remains were reviewed and approved by the Ethical Committee of Xiamen University. All necessary permissions for sampling and analysis were obtained from the Shandong Provincial Institute of Cultural Relics and Archaeology. Furthermore, prior to destructive sampling, the research team conducted consultations with local Hui community representatives and obtained their consent to proceed with the study, ensuring that all genomic analyses were conducted in a culturally and ethically responsible manner.

References

Alacamli ET, Naidoo T, Guler MN, Saglican E, Akturk S, Mapelli I, Vural KB, Somel M, Malmstrom H, Gunther T (2024) READv2: advanced and user-friendly detection of biological relatedness in archaeogenomics. Genome Biol 25:216

Alexander DH, Novembre J, Lange K (2009) Fast model-based estimation of ancestry in unrelated individuals. Genome Res 19:1655–1664

Allen, E., Yu, Y., Yang, X., Xu, Y., Du, P., Xiong, J., Chen, D., Tian, X., Wu, Y., Qin, X., Sheng, P., Wang, C.-C., & Wen, S. (2022). Multidisciplinary lines of evidence reveal East/Northeast Asian origins of agriculturalist/pastoralist residents at a Han dynasty military outpost in ancient Xinjiang. Frontiers in Ecology and Evolution, Volume 10 - 2022.

Chen, L. (1999) Zhongguo minzushi gangyao (The compendium of Chinese nationality histories).

Chintalapati, M., Patterson, N., & Moorjani, P. (2022). The spatiotemporal patterns of major human admixture events during the European Holocene. Elife, 11.

Cooke NP, Mattiangeli V, Cassidy LM, Okazaki K, Stokes CA, Onbe S, Hatakeyama S, Machida K, Kasai K, Tomioka N, Matsumoto A, Ito M, Kojima Y, Bradley DG, Gakuhari T, Nakagome S (2021) Ancient genomics reveals tripartite origins of Japanese populations. Sci Adv 7:eabh2419

de Flamingh A, Coutu A, Roca AL, Malhi RS (2020) Accurate sex identification of ancient elephant and other animal remains using low-coverage DNA shotgun sequencing data. G3 (Bethesda) 10:1427–1432

Du P, Zhu K, Wang M, Sun Z, Tan J, Sun B, Sun B, Wang P, He G, Xiong J, Huang Z, Meng H, Sun C, Xie S, Wang B, Ge D, Ma Y, Sheng P, Ren X, Tao Y, Wen S (2024) Genomic dynamics of the lower yellow river valley since the early neolithic. Curr Biol 34:3996-4006 e11

Fang H, Liang F, Ma H, Wang R, He H, Qiu L, Tao L, Zhu K, Wu W, Ma L, Zhang H, Chen S, Zhu C, Chen H, Xu Y, Zhao Y, Liu H, Wang CC (2025) Dynamic history of the Central Plain and Haidai region inferred from Late Neolithic to Iron Age ancient human genomes. Cell Rep 44(2):115262

Frachetti, M. (2013). Bronze age pastoralism and differentiated landscapes along the Inner Asian Mountain Corridor. Connections and Complexity: New Approaches to the Archaeology of South Asia, 279–298.

Fu Q, Mittnik A, Johnson PLF, Bos K, Lari M, Bollongino R, Sun C, Giemsch L, Schmitz R, Burger J, Ronchitelli AM, Martini F, Cremonesi RG, Svoboda J, Bauer P, Caramelli D, Castellano S, Reich D, Paabo S, Krause J (2013) A revised timescale for human evolution based on ancient mitochondrial genomes. Curr Biol 23:553–559

Ginolhac A, Rasmussen M, Gilbert MTP, Willerslev E, Orlando L (2011) MapDamage: testing for damage patterns in ancient DNA sequences. Bioinformatics 27:2153–2155

Gladney, D. C. (1998) Ethnic identity in China: the making of a Muslim minority nationality.

He H, Kong X, Tao L, Zhu L, Wang X, Xu M, Chen Y, Zhu K, Xu Y, Chen H, Ma H, Wang R, Yang X, Bai T, Guo J, Yang Y, Jia

X, Wang CC (2025) Genetic stability in the lower Yangtze River basin from Song to Qing dynasty. BMC Biol 23(1):270

Jagadeesan A, Ebenesersdottir SS, Guethmundsdottir VB, Thordardottir EL, Moore KHS, Helgason A (2021) HaploGrouper: a generalized approach to haplogroup classification. Bioinformatics 37:570–572

Jeong C, Wang K, Wilkin S, Taylor WTT, Miller BK, Bemmann JH, Stahl R, Chiovelli C, Knolle F, Ulziibayar S, Khatanbaatar D, Erdenebaatar D, Erdenebat U, Ochir A, Ankhsanaa G, Vanchigdash C, Ochir B, Munkhbayar C, Tumen D, Kovalev A, Kradin N, Bazarov BA, Miyagashev DA, Konovalov PB, Zhambaltarova E, Miller AV, Haak W, Schiffels S, Krause J, Boivin N, Erdene M, Hendy J, Warinner C (2020) A dynamic 6,000-year genetic history of Eurasia's Eastern Steppe. Cell 183:890-904.e29

Ji Z, Chen K, Zheng J, Qin C, Cui S, Shen Q, Ma H, Wang B, Mao X, Liu Y, Zhou H, Zou X, Wang X, Tang J, Ma T, Wan W, Zhu K, Tao L, He H, Wang R, Wang CC (2025) Genomic formation of lower yellow river populations in the Han dynasty. BMC Biol 23(1):260

Jun G, Wing MK, Abecasis GR, Kang HM (2015) An efficient and scalable analysis framework for variant extraction and refinement from population-scale DNA sequence data. Genome Res 25:918–925

Knapp M, Clarke A, Horsburgh K, Matisoo-Smith L (2011) Setting the stage - building and working in an ancient DNA laboratory. Ann Anat 194:3–6

Knapp M, Clarke AC, Horsburgh KA, Matisoo-Smith EA (2012) Setting the stage - building and working in an ancient DNA laboratory. Ann Anat 194:3–6

Korneliussen TS, Albrechtsen A, Nielsen R (2014) ANGSD: analysis of next generation sequencing data. BMC Bioinformatics 15:356

Kumar V, Wang W, Zhang J, Wang Y, Ruan Q, Yu J, Wu X, Hu X, Wu X, Guo W, Wang B, Niyazi A, Lv E, Tang Z, Cao P, Liu F, Dai Q, Yang R, Feng X, Ping W, Zhang L, Zhang M, Hou W, Liu Y, Bennett EA, Fu Q (2022) Bronze and Iron Age population movements underlie Xinjiang population history. Science 376:62–69

Li H, Durbin R (2010) Fast and accurate long-read alignment with Burrows-Wheeler transform. Bioinformatics 26:589–595

Li H, Handsaker B, Wysoker A, Fennell T, Ruan J, Homer N, Marth G, Abecasis G, Durbin R, Genome Project Data Processing (2009) The sequence alignment/map format and SAMtools. Bioinformatics 25:2078–2079

Li S, Wang R, Ma H, Tu Z, Qiu L, Chen H, Jiang L, Geng Y, Liu H, Wang J, Shen Q, Jin L, Li C, Wang CC, Wei X (2024) Ancient genomic time transect unravels the population dynamics of Neolithic middle Yellow River farmers. Sci Bull 69(21):3365–3370

Li H, Wang B, Yang X, Yang X, He H, Wang R, Wang CC (2025) Ancient genomes shed light on the genetic history of the Iron Age to historical central Xinjiang, northwest China. BMC Biol 23(1):93

Liu C (2023) New exploration on Sogdians and Sinicization in the Wei, Jin, Southern and Northern Dynasties—traces in traditional historical materials. Open Journal of Historical Studies 11:293–297

Llamas B, Valverde G, Fehren-Schmitz L, Weyrich LS, Cooper A, Haak W (2017) From the field to the laboratory: controlling DNA contamination in human ancient DNA research in the high-throughput sequencing era. STAR Sci Technol Archaeol Res 3:1–14

Loh PR, Lipson M, Patterson N, Moorjani P, Pickrell JK, Reich D, Berger B (2013) Inferring admixture histories of human populations using linkage disequilibrium. Genetics 193:1233–1254

Lv M, Ma H, Wang R, Li H, Zhang X, Zhang W, Zeng Y, Qin Z, Zhai H, Lou Y, Lin Y, Tao L, He H, Yang X, Zhu K, Zhou Y, Wang CC (2024) Ancient genomes from the Tang Dynasty capital reveal the genetic legacy of trans-Eurasian communication at the eastern end of Silk Road. BMC Biol 22:267

Ma H, Zhou Y, Wang R, Yan F, Chen H, Qiu L, Zhao J, Jin L, Wang CC (2025) Ancient genomes shed light on the long-term genetic stability in the Central Plain of China. Sci Bull (Beijing) 70:333–337

Mallick S, Micco A, Mah M, Ringbauer H, Lazaridis I, Olalde I, Patterson N, Reich D (2024) The Allen Ancient DNA Resource (AADR) a curated compendium of ancient human genomes. Sci Data 11:182

Mittnik A, Wang CC, Svoboda J, Krause J (2016) A Molecular Approach to the Sexing of the Triple Burial at the Upper Paleolithic Site of Dolni Vestonice. PLoS ONE 11:e0163019

Ning C, Li T, Wang K, Zhang F, Li T, Wu X, Gao S, Zhang Q, Zhang H, Hudson MJ, Dong G, Wu S, Fang Y, Liu C, Feng C, Li W, Han T, Li R, Wei J, Zhu Y, Zhou Y, Wang CC, Fan S, Xiong Z, Sun Z, Ye M, Sun L, Wu X, Liang F, Cao Y, Wei X, Zhu H, Zhou H, Krause J, Robbeets M, Jeong C, Cui Y (2020) Ancient genomes from northern China suggest links between subsistence changes and human migration. Nat Commun 11:2700

Nodirabegim V (2021) Sogdians in China: a phenomenon in history and culture in medieval China. Psychol Educ J 58:4956–4965

Patterson N, Moorjani P, Luo Y, Mallick S, Rohland N, Zhan Y, Genschoreck T, Webster T, Reich D (2012) Ancient admixture in human history. Genetics 192:1065–1093

Peltzer A, Jager G, Herbig A, Seitz A, Kniep C, Krause J, Nieselt K (2016) EAGER: efficient ancient genome reconstruction. Genome Biol 17:60

Purcell S, Neale B, Todd-Brown K, Thomas L, Ferreira MA, Bender D, Maller J, Sklar P, de Bakker PI, Daly MJ, Sham PC (2007) PLINK: a tool set for whole-genome association and population-based linkage analyses. Am J Hum Genet 81:559–575

Qiu L, Chen H, Chen H, Qin C, Xu M, Jiang Y, Ma H, Shen Q, Peng Y, Mao X, Liu Y, Wang B, Ji Z, Zhu K, Xu Y, Tao L, He H, Zhou H, Zou X, Wang X, Wang CC (2026) Reconstructing the genetic formation of Han Chinese from ancient genomes. BMC Biol 24(1):68

Ralf A, Gonzalez DM, Zhong K, Kayser M (2018) Yleaf: software for human Y-chromosomal haplogroup inference from next-generation sequencing data. Mol Biol Evol 35:1820

Ramsey CB, Lee S (2013) Recent and planned developments of the program OxCal. Radiocarbon 55:720–730

Renaud G, Slon V, Duggan AT, Kelso J (2015) Schmutzi: estimation of contamination and endogenous mitochondrial consensus calling for ancient DNA. Genome Biol 16:224

Ringbauer H, Novembre J, Steinrucken M (2021) Parental relatedness through time revealed by runs of homozygosity in ancient DNA. Nat Commun 12:5425

Robbeets M, Bouckaert R, Conte M, Savelyev A, Li T, An DI, Shinoda KI, Cui Y, Kawashima T, Kim G, Uchiyama J, Dolinska J, Oskolskaya S, Yamano KY, Seguchi N, Tomita H, Takamiya H, Kanzawa-Kiriyama H, Oota H, Ishida H, Kimura R, Sato T, Kim JH, Deng B, Bjorn R, Rhee S, Ahn KD, Gruntov I, Mazo O, Bentley JR, Fernandes R, Roberts P, Bausch IR, Gilaizeau L, Yoneda M, Kugai M, Bianco RA, Zhang F, Himmel M, Hudson MJ, Ning C (2021) Triangulation supports agricultural spread of the Transeurasian languages. Nature 599:616–621

Savelyev A, Robbeets M (2020) Bayesian phylolinguistics infers the internal structure and the time-depth of the Turkic language family. J Lang Evol 5:39–53

Schubert M, Lindgreen S, Orlando L (2016) AdapterRemoval v2: rapid adapter trimming, identification, and read merging. BMC Res Notes 9:88

Shen Q, Wu Z, Zan X, Yang X, Guo J, Ji Z, Wang B, Liu Y, Mao X, Wang X, Zou X, Zhou H, Peng Y, Ma H, He H, Bai T, Xu M, Wen S, Jin L, Zhang Q, Wang CC (2025) Ancient genomes illuminate the demographic history of Shandong over the past two millennia. J Genet Genomics 52:494–501

Sun L, Ma H, Wang R, Wu Z, Qiu L, Chen H, Wang CC (2025) The demic expansion of Yangshao culture inferred from ancient human genomes. BMC Biol 23(1):186

Tang J, Wang R, Wei Q, He H, Deng C, Tao L, Mao X, Ma H, Wang X, Zou X, Yang X, Zhang Q, Wu Q, Guo Y, Wang CC (2026) Social Stratification Without Genetic Differentiation at the Xisima Site in the Late Shang Dynasty. Mol Biol Evol 43(1):msaf316

Tao L, Yuan H, Zhu K, Liu X, Guo J, Min R, He H, Cao D, Yang X, Zhou Z, Wang R, Zhao D, Ma H, Chen J, Zhao J, Li Y, He Y, Suo D, Zhang R, Li S, Wang CC (2023) Ancient genomes reveal millet farming-related demic diffusion from the Yellow River into southwest China. Curr Biol: CB 33(22):4995-5002.e7

Tao L, Xie Y, He H, Bai T, Guo J, Zhu K, Wang B, Xie G, Lin Q, Wang CC (2026) Genetic formation and regional disparities of Kra-Dai and Hmong-Mien speakers inferred from ancient genomes of cave burial populations in southwest China. Mol Biol Evol 43(2):msag34

van Klinken GJ (1999) Bone collagen quality indicators for palaeodietary and radiocarbon measurements. J Archaeol Sci 26:687–695

Wan W, Huang H, Hu C, Zhang X, Zhou Q, Yang M, Guo J, Xie M, Zhu K, Yang X, Ma H, Wang R, Zhao J, Tao L, He H, Zhang Q, Jin L, Zhou B, Huang J, Wang CC (2025) Ancient genomes in Southwest China revealed genetic interactions among diverse populations in the historical period. BMC Biol 23(1):174

Wang CC, Yeh HY, Popov AN, Zhang HQ, Matsumura H, Sirak K, Cheronet O, Kovalev A, Rohland N, Kim AM, Mallick S, Bernardos R, Tumen D, Zhao J, Liu YC, Liu JY, Mah M, Wang K, Zhang Z, Adamski N, Broomandkhoshbacht N, Callan K, Candilio F, Carlson KSD, Culleton BJ, Eccles L, Freilich S, Keating D, Lawson AM, Mandl K, Michel M, Oppenheimer J, Özdoğan KT, Stewardson K, Wen S, Yan S, Zalzala F, Chuang R, Huang CJ, Looh H, Shiung CC, Nikitin YG, Tabarev AV, Tishkin AA, Lin S, Sun ZY, Wu XM, Yang TL, Hu X, Chen L, Du H, Bayarsaikhan J, Mijiddorj E, Erdenebaatar D, Iderkhangai TO, Myagmar E, Kanzawa-Kiriyama H, Nishino M, Shinoda KI, Shubina OA, Guo J, Cai W, Deng Q, Kang L, Li D, Li D, Lin R, Nini Shrestha R, Wang LX, Wei L, Xie G, Yao H, Zhang M, He G, Yang X, Hu R, Robbeets M, Schiffels S, Kennett DJ, Jin L, Li H, Krause J, Pinhasi R, Reich D (2021a) Genomic insights into the formation of human populations in East Asia. Nature 591:413–419

Wang T, Wang W, Xie G, Li Z, Fan X, Yang Q, Wu X, Cao P, Liu Y, Yang R, Liu F, Dai Q, Feng X, Wu X, Qin L, Li F, Ping W, Zhang L, Zhang M, Liu Y, Chen X, Zhang D, Zhou Z, Wu Y, Shafiey H, Gao X, Curnoe D, Mao X, Bennett EA, Ji X, Yang MA, Fu Q (2021b) Human population history at the crossroads of East and Southeast Asia since 11,000 years ago. Cell 184:3829-3841 e21

Wang H, Yang MA, Wangdue S, Lu H, Chen H, Li L, Dong G, Tsring T, Yuan H, He W, Ding M, Wu X, Li S, Tashi N, Yang T, Yang F, Tong Y, Chen Z, He Y, Cao P, Dai Q, Liu F, Feng X, Wang T, Yang R, Ping W, Zhang Z, Gao Y, Zhang M, Wang X, Zhang C, Yuan K, Ko AM, Aldenderfer M, Gao X, Xu S, Fu Q (2023) Human genetic history on the Tibetan Plateau in the past 5100 years. Sci Adv 9:eadd5582

Wang B, Hao D, Xu Y, Zhu K, Wang R, Yang X, Shen Q, Xu M, Bai T, Ma H, Zheng J, Wang X, Zou X, Zhou H, Mao X, Tang J, Peng Y, Tao L, He H, Chen H, Wang CC (2024a) Population expansion from central plain to northern coastal China inferred from ancient human genomes. iScience 27(12):111405

Wang F, Wang R, Ma H, Zeng W, Zhao Y, Wu H, Tang Z, He H, Fang H, Wang CC (2024b) Neolithization of Dawenkou culture in the lower Yellow River involved the demic diffusion from the Central Plain. Sci Bull 69(23):3677–3681

Wang R, Liu W, Wu Y, Ma H, Lv J, He H, Qiu L, Chen H, Zhao Y, Sun B, Wang CC (2025a) East and West admixture in eastern China of Tang Dynasty inferred from ancient human genomes. Commun Biol 8:219

Wang R, Zhu L, Ma H, Song M, Ma G, Wang B, Fu L, Hao J, Fu G, Wang J, Wang Q, Zhu K, Yang X, Xu Y, Tao L, He H, Li S, Jiang J, Zhang W, Wang CC, Cong B (2025b) Genetic formation of Neolithic Hongshan people and demic expansion of Hongshan culture inferred from ancient human genomes. Mol Biol Evol 42(6):msaf139

Weissensteiner H, Pacher D, Kloss-Brandstatter A, Forer L, Specht G, Bandelt HJ, Kronenberg F, Salas A, Schonherr S (2016) HaploGrep 2: mitochondrial haplogroup classification in the era of high-throughput sequencing. Nucleic Acids Res 44:W58-63

Xiong J, Wang R, Chen G, Yang Y, Du P, Meng H, Ma M, Allen E, Tao L, Wang H, Jin L, Wang CC, Wen S (2024) Inferring the demographic history of Hexi Corridor over the past two millennia from ancient genomes. Sci Bull (Beijing) 69:606–611

Xiong J, Xu Y, Chen G, Yang L, Zhou Y, Pan Y, Wang Z, Bai J, Zhang B, Dong G, Pei J, Yang X, Chen L, Kang N, Wu Y, Wang B, Zhu K, Du P, Li X, Wen H, Wen S (2025) The genomic history of East Asian Middle Neolithic millet- and rice-agricultural populations. Cell Genomics 5(10):100976

Xue Z, Sun R, Li C, Cui Y (2025) Genetic history of ancient Xinjiang revealed by ancient DNA study: a hub of Eurasian population migration and cultural exchange. Nat Anthropol 3:10010–10010

Yang Q (1999) Ritual and custom culture of Chinese Muslims. Ningxia People's Publishing House

Yang MA, Fan X, Sun B, Chen C, Lang J, Ko YC, Tsang CH, Chiu H, Wang T, Bao Q, Wu X, Hajdinjak M, Ko AM, Ding M, Cao P, Yang R, Liu F, Nickel B, Dai Q, Feng X, Zhang L, Sun C, Ning C, Zeng W, Zhao Y, Zhang M, Gao X, Cui Y, Reich D, Stoneking M, Fu Q (2020) Ancient DNA indicates human population shifts and admixture in northern and southern China. Science 369:282–288

Yang X, Zou X, Li H, Yang X, Wang B, Ma H, Wang Y, Xu Y, Li C, Wang CC (2026) Ancient genomes uncover dynamic cultural and genetic interplay in the eastern Tianshan. Mol Biol Evol 43(3):msag057

Yang, X., Li, H., Wang, B., Zhu, K., Haifeng, H., Ji, Z., Wang, B., Zhao, J. & Wang, C. C. (2025). Population dynamics in Iron Age Xinjiang inferred from ancient genomes of the Zhagunluke site. Archaeol Anthropol Sci 17.

Yao H, Wang M, Zou X, Li Y, Yang X, Li A, Yeh HY, Wang P, Wang Z, Bai J, Guo J, Chen J, Ding X, Zhang Y, Lin B, Wang CC, He G (2021) New insights into the fine-scale history of western-eastern admixture of the northwestern Chinese population in the Hexi Corridor via genome-wide genetic legacy. Mol Genet Genomics 296:631–651

Ying-sheng L (2003) A brief review of the 800-year development history of Hui language: from Persian to "Hui Chinese." China Culture Research 4:143–153

Zhang F, Ning C, Scott A, Fu Q, Bjorn R, Li W, Wei D, Wang W, Fan L, Abuduresule I, Hu X, Ruan Q, Niyazi A, Dong G, Cao P, Liu F, Dai Q, Feng X, Yang R, Tang Z, Ma P, Li C, Gao S, Xu Y, Wu S, Wen S, Zhu H, Zhou H, Robbeets M, Kumar V, Krause J, Warinner C, Jeong C, Cui Y (2021) The genomic origins of the Bronze Age Tarim Basin mummies. Nature 599:256–261

Zhou H, Tao L, Zhao Y, He H, Shi H, Yu T, Guo Y, He Y, Liu H, Wu Y, Cao J, Kuang Z, Wu S, Lin F, Yang Y, Xiong L, Liu Y, Zhu K, Xu Y, Huang S, Zhang X (2025) Exploration of hanging coffin customs and the bo people in China through comparative genomics. Nat Commun 16(1):10230

Zhou Y, Lin Y, Ma H, Wang R, Zhai H, Qin Z, Zeng Y, Lou Y, Xu Y, Chen H, Bai T, Shen W, Chen T, Yang X, Zheng J, Tao L, He H, Zhu K, Li J, Chen L, Wang CC (2026) Ancient genomes from the Qing Dynasty reveal unbroken genetic continuity in China's Central Plains. Mol Biol Evol 43(1):msaf335

Zhu S, Ding P, Wang N, Shen C, Jia GB, Zhang G (2015) The compact AMS facility at Guangzhou Institute of Geochemistry, Chinese Academy of Sciences. Nuclear Instruments & Methods in Physics

Research Section B-Beam Interactions with Materials and Atoms 361:72–75

Zhu K, Du P, Li J, Zhang J, Hu X, Meng H, Chen L, Zhou B, Yang X, Xiong J, Allen E, Ren X, Ding Y, Xu Y, Chang X, Yu Y, Han S, Dong G, Wang CC, Wen S (2022) Cultural and demic co-diffusion of Tubo Empire on Tibetan Plateau. iScience 25(12):105636

Zhu K, He H, Tao L, Ma H, Yang X, Wang R, Guo J, Wang CC (2024a) Protocol for a comprehensive pipeline to study ancient human genomes. STAR Protoc 5:102985

Zhu K, Hu C, Yang M, Zhang X, Guo J, Xie M, Yang X, Ma H, Wang R, Zhao J, Tao L, He H, Wan W, Zhang Q, Jin L, Zuo Y, Zhou B, Huang J, Wang CC (2024b) The demic diffusion of Han culture into the Yunnan-Guizhou plateau inferred from ancient genomes. Natl Sci Rev 11(12):nwae387